Dynamin 2 mutations in Charcot–Marie–Tooth neuropathy highlight the importance of clathrin-mediated endocytosis in myelination

Páris N. M. Sidiropoulos,[1] Michaela Miehe,[1] Thomas Bock,[2,3] Elisa Tinelli,[1] Carole I. Oertli,[1] Rohini Kuner,[4] Dies Meijer,[5] Bernd Wollscheid,[2,3] Axel Niemann[1,*] and Ueli Suter[1,*]

1 Department of Biology, Institute of Molecular Health Sciences, Chair in Cell Biology, ETH Zurich, CH-8093 Zurich, Switzerland
2 Department of Biology, Institute of Molecular Systems Biology, ETH Zurich, CH-8093 Zurich, Switzerland
3 National Centre of Competence in Research (NCCR)–Neuro Centre for Proteomics, UZH/ETH Zurich, CH-8093 Zurich, Switzerland
4 Institute for Pharmacology, Heidelberg University, D-69120 Heidelberg, Germany
5 Department of Cell Biology and Genetics, Erasmus University Medical Centre, 3000 CA Rotterdam, The Netherlands

*These authors contributed equally to this work

Correspondence to: Prof. Dr. Ueli Suter,
Institute of Molecular Health Sciences, Chair in Cell Biology,
ETH Zurich, ETH-Hönggerberg, HPM E39,
Schafmattstrasse 18,
CH-8093 Zurich, Switzerland
E-mail: usuter@cell.biol.ethz.ch

Mutations in dynamin 2 (*DNM2*) lead to dominant intermediate Charcot–Marie–Tooth neuropathy type B, while a different set of *DNM2* mutations cause autosomal dominant centronuclear myopathy. In this study, we aimed to elucidate the disease mechanisms in dominant intermediate Charcot–Marie–Tooth neuropathy type B and to find explanations for the tissue-specific defects that are associated with different *DNM2* mutations in dominant intermediate Charcot–Marie–Tooth neuropathy type B versus autosomal dominant centronuclear myopathy. We used tissue derived from *Dnm2*-deficient mice to establish an appropriate peripheral nerve model and found that dominant intermediate Charcot–Marie–Tooth neuropathy type B-associated dynamin 2 mutants, but not autosomal dominant centronuclear myopathy mutants, impaired myelination. In contrast to autosomal dominant centronuclear myopathy mutants, Schwann cells and neurons from the peripheral nervous system expressing dominant intermediate Charcot–Marie–Tooth neuropathy mutants showed defects in clathrin-mediated endocytosis. We demonstrate that, as a consequence, protein surface levels are altered in Schwann cells. Furthermore, we discovered that myelination is strictly dependent on Dnm2 and clathrin-mediated endocytosis function. Thus, we propose that altered endocytosis is a major contributing factor to the disease mechanisms in dominant intermediate Charcot–Marie–Tooth neuropathy type B.

Introduction

Charcot-Marie-Tooth disease (CMT), also called hereditary motor and sensory neuropathy, is one of the most common monogenetic diseases of the nervous system (Skre, 1974). CMT is clinically and genetically diverse (for further information see http://neuromuscular.wustl.edu/time/hmsn.html) and has been classified by electrophysiological and histopathological means into demyelinating or dysmyelinating (CMT1, CMT3, CMT4) and axonal forms (CMT2) (Dyck *et al.*, 1993). Axonal CMT shows slightly reduced to normal nerve conduction velocity, but reduced compound muscle action potential due to major loss of myelinated axons. Cellular effects of disease mutations leading to axonal forms are thought to originate on the neuronal side, whereas demyelinating or dysmyelinating CMT is generally assumed to start with an insult affecting myelinating Schwann cells. Characteristic for the myelin-affecting forms is decreased nerve conduction velocity, followed by axonal degeneration and reduced compound muscle action potential as the main correlate to clinical disability (Suter and Scherer, 2003; Scherer *et al.*, 2008).

Intermediate forms of CMT have also been described (Nicholson *et al.*, 2006) with uncertainty of whether these are primarily demyelinating or axonal disorders, or both. Within this group, dynamin 2 (*DNM2*) mutations have been linked to dominant-intermediate CMT subtype B (Zuchner *et al.*, 2005). Patients with dominant-intermediate CMT subtype B are characterized by mildly reduced nerve conduction velocity, loss of myelinated axons, rare segmental demyelination and remyelination with onion bulb formation, and focal hypermyelination (Zuchner *et al.*, 2005). The contributions of mutated forms of Dnm2 to the disease in neurons, in Schwann cells, and in the crucial dynamics of Schwann cell–axon interactions, are unclear (Nicholson *et al.*, 2006; Claeys *et al.*, 2009).

Dynamins are highly conserved, large GTPases that belong to the dynamin superfamily (Heymann *et al.*, 2009). In general, they hydrolyze GTP enabling them to act as mechanochemical proteins to mediate, or contribute to, membrane fission. The core group of classical dynamins consists of the three isoforms: Dnm1, Dnm2 and Dnm3. In addition, the family of large GTPases includes the subfamily of dynamin-related proteins with mitofusin 2 (CMT2A causing gene) and OPA1 (mutated in autosomal dominant optic atrophy) as prominent members. Classical dynamins share a highly conserved catalytic N-terminal GTPase domain, a middle domain important for oligomerization, a pleckstrin homology domain critical for the interaction with membrane phosphoinositides and the regulation of GTPase activity (Kenniston *et al.*, 2010), and a GTPase effector domain, which is thought to act as GTPase activating-domain upon assembly of dynamin oligomers into higher order structures (Ramachandran, 2007). The less well-conserved C-terminus contains an arginine-/proline-rich domain, which is a major partner for interacting proteins (Durieux *et al.*, 2010) (Fig. 1). The vast majority of CMT-associated *DNM2* mutations are clustered in the N-terminal part of the pleckstrin homology domain (Fig. 1).

A second distinct set of *DNM2* mutations, mainly found in the middle domain and at the pleckstrin homology–GTPase effector domain boundary, is linked to autosomal-dominantcentronuclear myopathy (Kenniston *et al.*, 2010) (Fig. 1). Autosomal-dominant centronuclear myopathy (CNM) is characterized by slowly progressive muscular weakness and wasting with centrally located nuclei in a large number of skeletal muscle fibres, radial arrangement of sarcoplasmic strands and predominance of hypotrophy of type 1 fibres (Fischer *et al.*, 2006; http://neuromuscular.wustl.edu/musdist/distal.html#distal).

Dnm2 is ubiquitously expressed and is involved in several cellular processes including various endocytotic pathways, vesicle trafficking from and to the *trans*-Golgi network, centrosome cohesion and actin- and microtubular dynamics (Praefcke *et al.*, 2004; Liu *et al.*, 2008; Ferguson *et al.*, 2009). The three classical dynamin isoforms share some functions and individual members can, at least partially, compensate for each other, while other functions are unique (Ferguson *et al.*, 2007, 2009; Liu *et al.*, 2008; Durieux *et al.*, 2010). However, Dnm1 expression is largely restricted to neuronal cells, and Dnm3 is found in brain, heart, lung and testis. At the organism level, *Dnm1*-deficient mice die within 2 weeks after birth and show poor motor coordination (Ferguson *et al.*, 2007). Furthermore, ablation of *Dnm1* correlates with severe impairment of synaptic vesicle reformation during intense activity. In contrast, ubiquitous deletion of *Dnm2* results in early embryonic lethality indicating a pivotal role of Dnm2 in early mouse development (Ferguson *et al.*, 2009; unpublished data).

The consequences of some mutations associated with CMT or CNM have been studied *in vitro* and in different model systems. *In vitro*, at least some CNM-associated *DNM2* mutants (CNM mutants) alter dynamin's GTPase activity, while retaining binding to phospholipids (Kenniston *et al.*, 2010). In contrast, Zuchner *et al.* (2005) proposed diminished binding to membranes of selected CMT-associated *DNM2* mutants (CMT mutants). Furthermore, several CNM mutants form abnormally stable polymers (Wang *et al.*, 2010). At the cellular level, interference with centrosome cohesion was suggested as potential disease mechanism for CNM mutants R369W and R465W, whereas expression of the CMT mutant D555_E557Δ resulted in altered microtubule dynamics and defects in mature Golgi complex formation (Zuchner *et al.*, 2005; Tanabe *et al.*, 2009).

A comparison of different mutants in Cos7 cells revealed inhibition of transferrin uptake upon expression of CNM mutants R465W, V625Δ, E650K and of CMT mutant K562E, whereas the CMT mutant D555_E557Δ had no impact (Bitoun *et al.*, 2009; Tanabe *et al.*, 2009). Impairment of clathrin-mediated endocytosis was also found in fibroblasts from a patient with CNM carrying the R465W mutant (Bitoun *et al.*, 2009). Despite these data, mouse embryonic fibroblasts with a heterozygous Dnm2 R465W knock-in mutation did not reveal a clathrin-mediated endocytosis defect, whereas homozygous cells did (Durieux *et al.*, 2010).

Notwithstanding recent progress on biochemical malfunctions caused by *DNM2* mutations (Kenniston *et al.*, 2010; Wang *et al.*, 2010), a thorough understanding of the disease mechanisms and the development of pathologies requires detailed analysis in appropriate cellular systems. We were particularly interested in addressing why and how CMT-causing *DNM2* mutations have
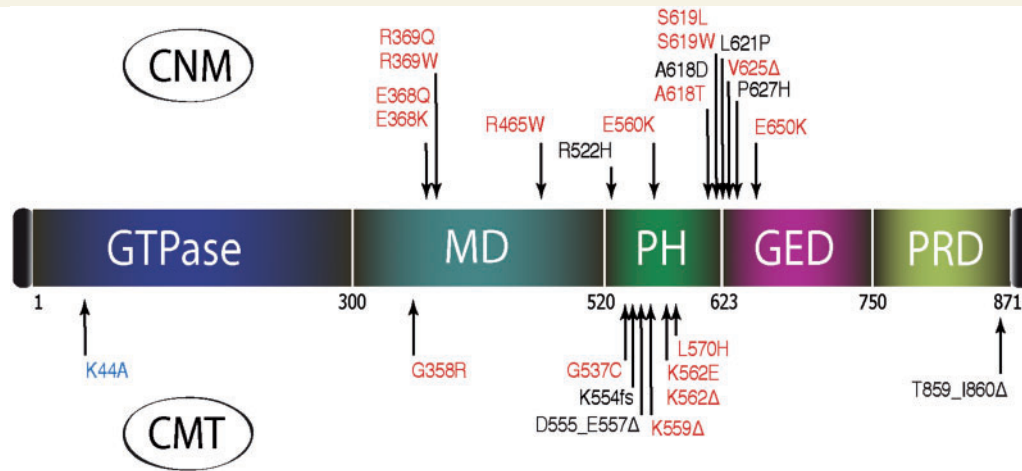
Figure 1 Dominant inherited mutations in *DNM2* that cause CMT or CNM. A schematic representation of the Dnm2 protein illustrates that *DNM2* mutations leading to dominant-intermediate CMT subtype B are mainly clustered in the N-terminal part of the pleckstrin homology (PH) domain. *DNM2* autosomal-dominant CNM mutations are localized within the middle domain (MD), pleckstrin homology domain and GTPase effector domain (GED). Mutations highlighted in red were cloned by site-directed mutagenesis and used in this article. The dominant-negative point mutation K44A (blue) within the GTPase domain leads to a catalytic-deficient protein and was used as control.

a selective deleterious effect on myelinated peripheral nerves. By comparing CMT- with CNM-causing mutants, we aimed to reveal disease-specific mechanistic differences and/or cell type-specific effects. Using lentiviral gene transfer in combination with dissociated dorsal root ganglia explant cultures from ubiquitous and cell type-specific *Dnm2*-deficient mice, we have established a peripheral nerve disease model. We demonstrate that CMT mutants, in contrast to CNM mutants, have a destructive effect by impairing myelination. In line with these results, we found that CMT mutants inhibit clathrin-mediated endocytosis in Schwann cells and differentiated motor neurons, whereas CNM mutants do not. Indeed, clathrin-mediated endocytosis was found to be essential for peripheral nerve myelination and altered clathrin-mediated endocytosis appears to be a major contributor to the disease mechanism underlying dominant-intermediate CMT subtype B.

Materials and methods

Mice

Analysis of transgenic mice with exon 2 of *Dnm2* flanked by LoxP sites will be described elsewhere. Dnm2$^{wt/0}$ mice were generated using a Cre deleter mouse line. Mice heterozygous (Dnm2$^{wt/flox}$) or homozygous (Dnm2$^{flox/flox}$) for the *Dnm2* floxed allele were crossed with established mouse lines expressing Cre recombinase under the control of desert hedgehog (Dhh) (Jaegle *et al*., 2003) or Na$_V$1.8 sodium channel (SNS) (Agarwal *et al*., 2004) gene regulatory elements. Genotypes of mice were determined by polymerase chain reaction on genomic DNA derived from ear biopsies using *Dnm2*- and Cre-specific primer pairs (Supplementary material). Experiments with animals followed approved protocols (Veterinary Office, Canton Zurich, Switzerland).

Plasmids

Rat Dnm2 (in the splice form denoted aa) was kindly provided by Dr Ari Helenius (ETH Zurich, Switzerland). Dnm2 CMT and CNM disease-causing mutations (Fig. 1) were generated by site-directed mutagenesis (QuikChange® mutagenesis kit, Stratagene; for primers, see Supplementary material). Constructs were cloned into the enhanced green fluorescent protein (EGFP) vector pEGFP-N$_1$ (Clontech) or the lentiviral vector pSicoR-GFP (Addgene) for eukaryotic expression. Rat Dnm2 K44A-EGFP (splice form aa) was a kind gift from Dr Sandra Schmid (Scripps Research Institute, La Jolla, USA) and rat EGFP-tagged Dnm1 (splice form aa) and Dnm3 (in the splice form denoted aaa) were kindly supplied by Dr Marc McNiven (Mayo Clinic, Rochester, USA). All dynamin constructs used in this study were N-terminally tagged with EGFP. Short hairpin RNAs targeting clathrin heavy chain and AP-2 subunit μ2 (AP50) were from Sigma and subcloned into the Ubc-TurboGFP^{TM} vector (Sigma).

Antibodies and labelled transferrin

Primary antibodies used were: mouse monoclonal anti-Glycerinaldehyd-3-phosphat-Dehydrogenase (GAPDH; Hytest) mouse monoclonal anti-α-tubulin (Sigma), rat monoclonal anti-myelin basic protein (MBP; Serotec), mouse monoclonal anti-neurofilament medium chain (NF-160; Sigma), mouse monoclonal anti-AP50 (Becton Dickinson), mouse monoclonal anti-transferrin receptor (Serotec), rabbit polyclonal anti-ErbB2 (Abcam), rabbit polyclonal anti-integrin β$_1$ (Abcam), mouse monoclonal anti-Sox10 (R&D Systems), mouse monoclonal anti-Tuj-1 (Lucerna Chem). Secondary antibodies and detection reagents: horseradish peroxidase-conjugated goat anti-mouse, goat anti-rabbit and alakaline phosphatase-conjugated goat anti-mouse IgG (all Promega) for immunoblotting. Alexa Fluor 488 (Molecular Probes), Cy3-coupled streptavidin, Cy3 and Cy5-conjugated goat anti-rabbit, anti-rat and anti-mouse IgG antibodies (Jackson ImmunoResearch) for immunocytochemistry. Alexa Fluor 555- and Alexa Fluor 647-coupled transferrin were from Invitrogen.

Cell culture and transfections

HEK293T, HeLa cells, proliferating NSC-34 and RT4-D6P2T (RT4) cells were cultured in Dulbecco's modified Eagle medium with GlutaMAX^{TM} (Invitrogen) supplemented with 10% foetal calf serum (Brunswick). Culture medium for primary rat Schwann cells additionally contained 4 µg/ml glial growth factor (Harlan) and 8.2 µg/ml forskolin (Sigma). Differentiation of NSC-34 cells was induced by Dulbecco's modified Eagle medium/Ham's F12 supplemented with 1% foetal calf serum and 1% minimum essential medium-non-essential amino acids. Lipofectamine® 2000 (Invitrogen) and FugGENE® 6 (Roche) were used according to manufacturers' protocols.

Lentiviral stocks

High-titre lentivirus was produced as described (Stendel *et al.*, 2010). Additionally, lentivirus was titrated in HEK293T cells to obtain optimal transduction efficiencies. Primary Schwann cells, purified dorsal root ganglia neurons and dorsal root ganglia explant cultures were infected using 1.0×10^8 TU/ml of high-titre lentivirus, if not indicated differently.

Immunochemistry and microscopy

Cells were fixed with 4% paraformaldehyde in phosphate-buffered saline for 20 min at room temperature in the dark, washed with phosphate-buffered saline and permeabilized with 0.2% Triton X-100 (Sigma), blocked with phosphate-buffered saline containing 10% goat serum for 1 h at room temperature, followed by incubation with primary antibodies in blocking buffer for an additional hour at room temperature. After washing with phosphate-buffered saline, cells were incubated with fluorescent antibodies in blocking buffer for 1 h at room temperature. Cells were washed with phosphate-buffered saline, if indicated incubated for 5 min with 4′,6′-diamidino-2-phenylindole dihydrochloride (DAPI) (Sigma), washed again and mounted on coverslips (Immu-Mount; Thermo Scientific). Images were generated with an epifluorescence Zeiss Axioplan microscope equipped with a Zeiss MRM camera or a confocal inverted microscope (Leica SP2-AOBS) using argon and helium/neon lasers. Images were imported to Photoshop CS4 (Adobe) for appropriate pseudo-colouring, linear contrast adjustment, cropping and merging.

Dorsal root ganglia explant cultures

Dissociated dorsal root ganglia explant cultures were generated, allowed to myelinate, processed for immunochemistry, and quantified as described previously (Stendel *et al.*, 2010). Transduction efficiency was monitored by EGFP fluorescence. Quantification of myelination: at least nine fields per coverslip were randomly acquired (×10 magnification) and mean Cy3 fluorescence representing the myelin basic protein-positive segments was determined within the field of view using ImageJ software (National Institute of Health). Cy3-fluorescence of pSicoR-GFP control-infected dorsal root ganglia explant cultures was set to 100%. Results of wild-type-infected cultures were compared with cultures expressing Dnm2 mutant proteins. In rescue experiments, wild-type conditions were set to 100%. Experiments were done in independent triplicates and at least two coverslips per condition were analysed in each experiment.

Surface biotinylation and immunoblotting analysis

Cells were cooled on ice for 5 min and washed with phosphate-buffered saline. Biotin-3-sulpho-*N*-hydroxy succinimide (Sigma) was dissolved in water (1 mg/100 µl) and 2 ml cold phosphate-buffered saline including 100 µl biotin was added per plastic 35 mm cell culture dish (Nunc). Cells were incubated for 30 min on ice while gently shaking, washed with phosphate-buffered saline and unbound biotin was quenched with cold 0.1 M glycine in phosphate-buffered saline for 5 min. Subsequently, cells were lysed with RIPA buffer (50 mM Tris–HCl pH 7.4, 150 mM NaCl, 0.1% sodium dodecyl sulphate, 1% NP-40, 0.5% deoxycholic acid, 5 mM EDTA) containing protease inhibitor cocktail (Sigma), scraped off and sonicated. Cell lysates were recovered after centrifugation and incubated with streptavidin-coupled sepharose beads (GE Healthcare) overnight at 4°C. After intensive washing, the beads were boiled in sodium dodecyl sulphate sample buffer (80 mM Tris–HCl pH 6.8, 10% glycerol, 2% sodium dodecyl sulphate, 0.005% bromophenol blue), resolved by sodium dodecyl sulphate–polyacrylamide gel electrophoresis and immunoblotted on polyvinylidene fluoride transfer membranes (Millipore). Immunoblots were incubated with primary antibodies of interest followed by horseradish peroxidase or alkaline phosphatase chemiluminescence detection. Protein levels on western blots were quantified by densitometry using Quantity One® software (BioRad).

Transferrin assay for fluorescence-activated flow cytometry

RT4 cells were transfected with expression constructs and incubated in growth medium for 24 h. NSC-34 cells were additionally differentiated for 72 h. Subsequently, cells were serum-starved for 30 min at 37°C, followed by incubation with 8.4 µg/ml Alexa Fluor 647-labelled transferrin in serum-free Dulbecco's modified Eagle medium for 15 min at 37°C. Cells were washed, acid-stripped (0.2 M Na$_2$HPO$_4$, 0.1 M citric acid), detached with 0.25% trypsin (Gibco) and fixed with 4% paraformaldehyde. After washing and pelleting, the cells were resuspended in phosphate-buffered saline containing 20 mM EDTA, 2% foetal calf serum and 0.002% NaN$_3$ and subjected to flow cytometry. If indicated, dynasore (kindly provided by Dr Ari Helenius) or its solvent ethanol was added during serum starvation and transferrin incubation. Data acquisition: FACSCalibur flow cytometer using CellQuest software (BD Biosciences). Fluorescence intensity of internalized transferrin was measured for 2000 GFP (green fluorescent protein)-positive cells. The results using cells with high GFP expression are shown, if not indicated otherwise.

Biosynthetic assay

Primary rat Schwann cells were transduced with lentiviral vectors for 96 h. Cells were starved in Dulbecco's modified Eagle medium lacking *L*-methionine/*L*-cysteine (Gibco) for 30 min before pulsing with 0.2 mCi/ml ^{35}S-*L*-methionine/*L*-cysteine in starvation medium for additional 20 min. If indicated, 120 µM dynasore, 10 µg/ml brefeldin A or 0.25% dimethyl sulphoxide were added. Cells were surface biotinylated followed by cell lysis in RIPA-buffer and incubation with streptavidin-coupled sepharose overnight at 4°C. Beads were washed, boiled in sample buffer and resolved by sodium dodecyl-polyacrylamide gel electrophoresis. Gels were dried and analysed by autoradiography (STORM-800 PhosphorImager; GE Healthcare).

Primary rat Schwann cell surface proteome analysis

Primary rat Schwann cells were grown to 90% density and 20 million cells were used. Cell-surface capturing technology was performed as described previously (Wollscheid et al., 2009; Hofmann et al., 2010). Briefly, cells were oxidized with sodium metaperiodate on the cell culture plate at room temperature in the dark for 10 min, scraped after removal of the oxidative reagent and labelled with biocytin hydrazide at room temperature for 1 h. Cells were mechanically lysed in cold hypotonic buffer, cell membranes enriched by ultracentrifugation, and solubilized by detergent lysis (0.1% RapiGest) and indirect sonication. Carbamidomethylation of cysteine-containing proteins was performed [reduction: 5 mM tris(2-carboxyethyl)phosphine (TCEP), alkylation: 10 mM iodoacetamide] prior to tryptic digestion into peptides. Biotin-labelled N-glycopeptides were affinity enriched using streptavidin and further released by enzymatic cleavage of the carbohydrate chain (PnGaseF). Desalted peptide mixtures (Ultra MicroTIP Columns, The Nest Group) were dried in a vacuum concentrator. Prior to analysis, peptides were solubilized in Liquid Chromatography-Mass Spectrometry (LC-MS) grade water supplemented with 2% acetonitrile and 0.1% formic acid.

Statistical analysis

Data shown represent the average and standard deviation of three independent experiments. Statistical significance was assessed using a two-tailed unpaired Student's t-test ($*P < 0.05$, $**P < 0.01$ or $***P < 0.0001$).

Results

CMT-associated Dnm2 mutants impair myelination whereas CNM-associated mutants do not

We used dorsal root ganglia cultures to assess functional effects of Dnm2 disease-causing mutations in a relevant peripheral nerve model. To this end, mouse embryonic Day 13.5 dorsal root ganglia were explanted, dissociated and infected with lentiviral vectors encoding either EGFP (pSicoR), EGFP-tagged wild-type Dnm2, the artificially generated GTPase-deficient Dnm2 K44A mutant, selected Dnm2 CMT mutants, or CNM mutants (Fig. 1). After induction of myelination, immunocytochemistry for neurofilaments (NF-160; neurons) and myelin basic protein (for myelin) was used for analyses (Stendel et al., 2010).

We chose to employ dorsal root ganglia explants derived from embryos carrying a heterozygous *Dnm2* null allele (Dnm2$^{wt/0}$) to mimic closely the genetic situation in affected patients who carry a wild-type and a mutant *DNM2* allele. In this setting, we found that expression of the CMT mutant K562E strongly reduced myelination (Fig. 2A). In contrast, expression of the CNM mutant E560K had no discernable effect, equivalent to uninfected (data not shown), control-infected (pSicoR) and wild-type-overexpressing cultures. To determine whether the observed impairment is common to CMT mutants, we expanded the analysis to the mutants G358R, G537C, K559$\triangle$, K562$\triangle$ and L570H.

Indeed, quantitative analysis revealed that all but the K562$\triangle$ mutation affected myelination (Fig. 2B). Also Dnm2 K44A strongly impaired myelination, but both CNM mutants tested (R465W and E560K) had no significant effect.

To test the demyelinating potential of different mutants (Woodhoo et al., 2009), we infected robustly myelinated dorsal root ganglia explant cultures of Dnm2$^{wt/0}$ embryos with appropriate recombinant lentiviral vectors. Cultures were kept for an additional 8 days after the start of infection, and myelin was subsequently assessed by MBP immunostaining. Expression of the CMT mutant K562E led to myelin damage and induced myelin loss, in contrast to the CNM mutant E560K, control-infection (pSicoR) and wild-type-overexpression (Fig. 3A). Quantitative analysis revealed reduced myelin in cultures expressing Dnm2 K44A or both tested CMT mutants (G358R, K562E), whereas expression of the CNM mutant E560K had no detectable effect (Fig. 3B).

In our experiments, we found an effect on myelin formation and maintenance but no apparent alterations in Schwann cell numbers, neuronal survival or axonal outgrowth (data not shown). To check for potential effects of Dnm2 mutants on neurons closer, Dnm2$^{wt/0}$ dorsal root ganglia neurons were purified and cultured. Expression of CMT mutants G358R, G537C, K562E, L570H or the CNM mutant E560K in these cultures did not result in neuritic beading or altered microtubule acetylation (Supplementary Fig. 1). We conclude that CMT mutants have no overt effects on neurons in our experimental setup.

In the course of carrying out the initial set of myelination experiments, we found unexpectedly that expression of the Dnm2 K44A mutant and the CMT mutant K562E had no effect in our model if dorsal root ganglia from Dnm2$^{wt/wt}$ embryos were used (Supplementary Fig. 2). These findings indicated that endogenous Dnm2 gene dosage, and presumably different Dnm2 protein expression levels, have a critical influence on the functional effects of CMT mutants. Thus, we performed a series of studies that were aimed at examining potential cell type-specific effects of partial, or full loss of Dnm2 in neurons or Schwann cells in this experimental context.

To address the impact of Dnm2 loss in dorsal root ganglia neurons, we used transgenic mice expressing Cre recombinase under the control of sensory neuron-specific Na$_V$1.8 (SNS) gene regulatory elements (Agarwal et al., 2004). Loss of protein was determined in purified neurons obtained from dorsal root ganglia of SNSCre$^+$; Dnm2$^{flox/flox}$ embryos by immunoblotting. Recombination was further confirmed in mixed dorsal root ganglia cultures by polymerase chain reaction (data not shown). First, we used heterozygous SNSCre$^+$; Dnm2$^{wt/flox}$ dorsal root ganglia cultures and lentiviral expression of Dnm2 mutants. No significantly altered myelination was observed for the Dnm2 K44A mutant, CMT mutants G358R, G537C, K559$\triangle$, K562E, K562$\triangle$, L570H and CNM mutants R465W and E560K (Fig. 4A and B), compared with control or wild-type overexpression. Note that these observations differ from our findings with Dnm2$^{wt/0}$ dorsal root ganglia, where most CMT mutants and the Dnm2 K44A mutant displayed deleterious effects (Fig. 2). Next, we ablated *Dnm2* completely in sensory neurons. SNSCre$^+$; Dnm2$^{flox/flox}$ dorsal root ganglia cultures displayed normal levels of myelination compared with
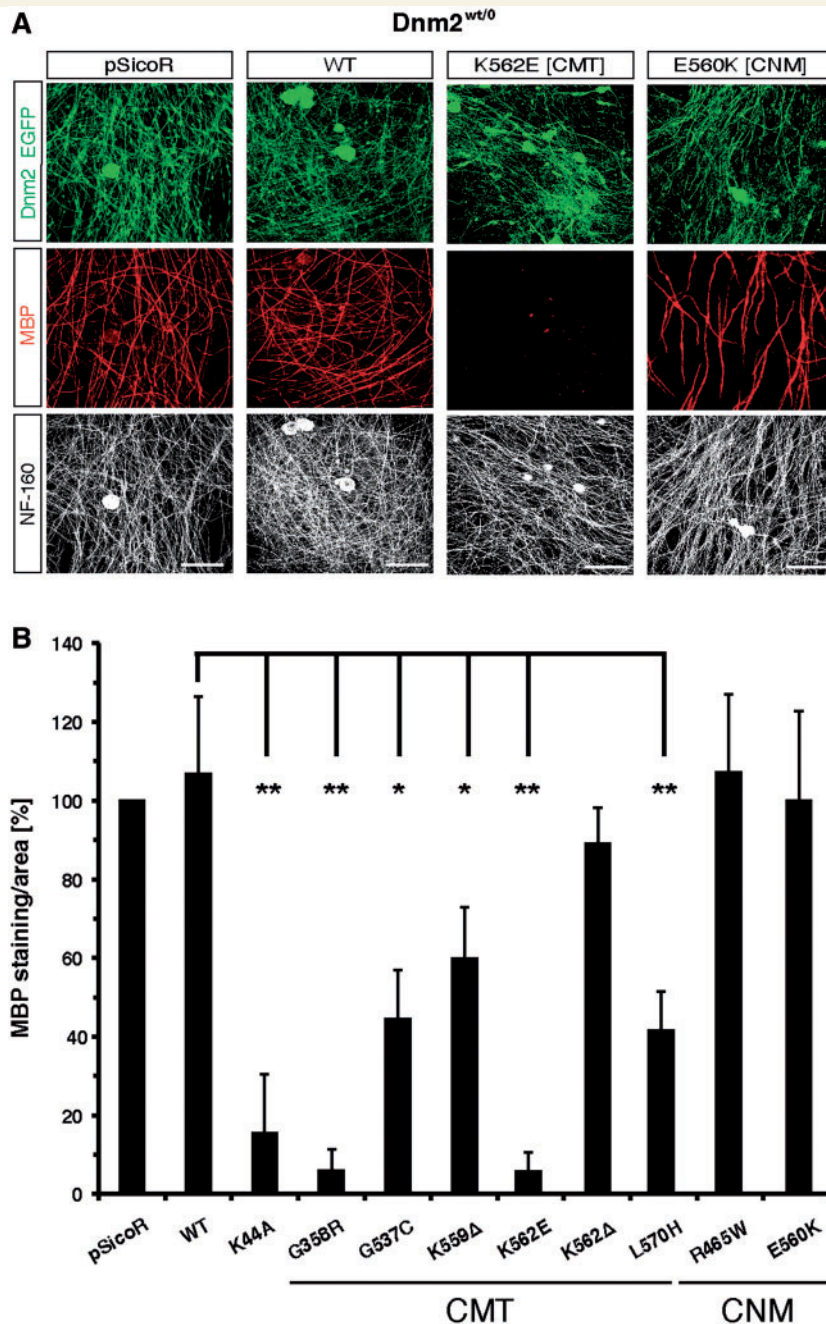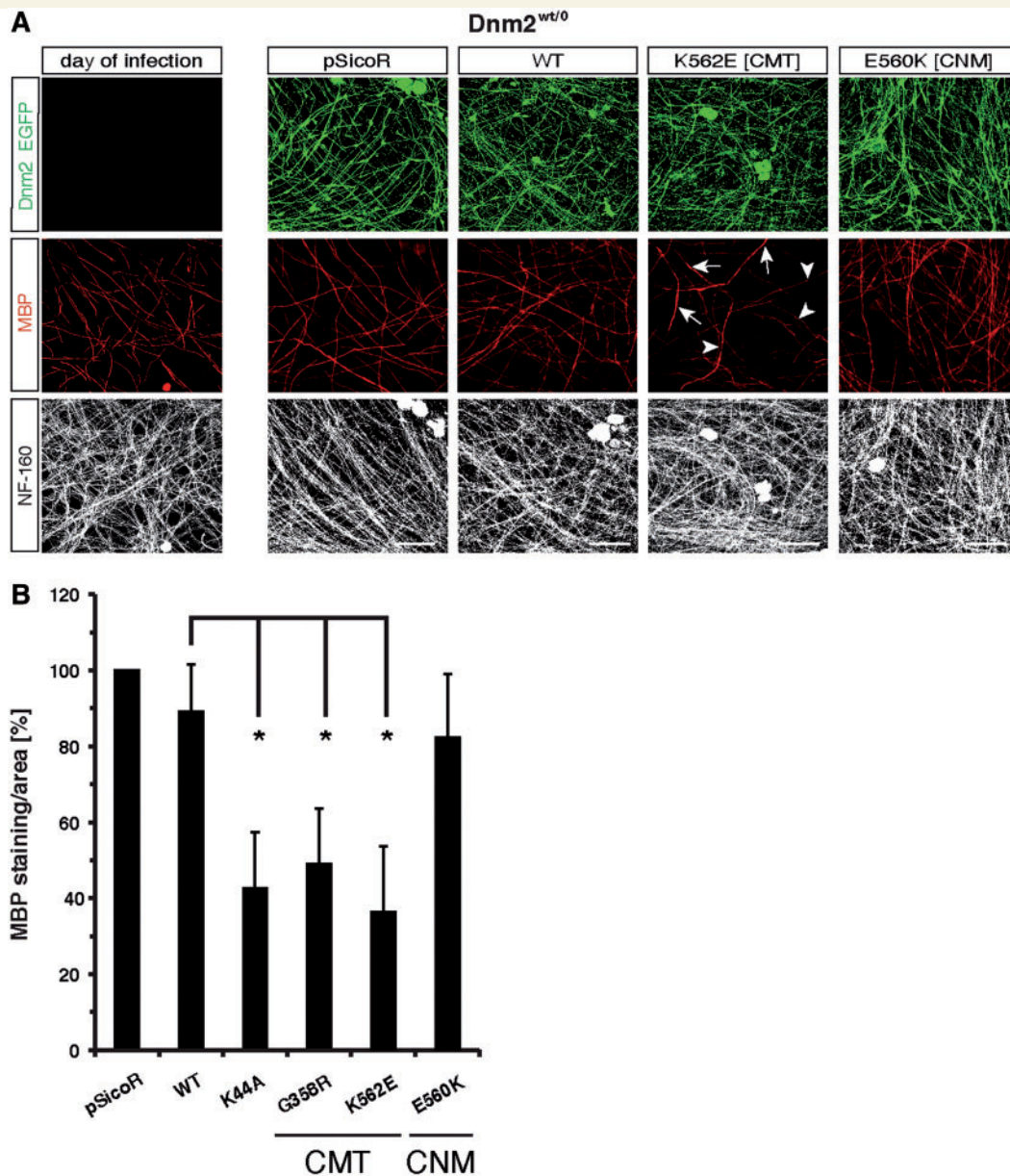
Figure 2 CMT-causing Dnm2 mutants impair myelination of heterozygous Dnm2$^{wt/0}$ dorsal root ganglia explant cultures. (**A**) Dorsal root ganglia explants dissected from Dnm2$^{wt/0}$ embryos were infected with lentivirus encoding GFP alone (pSicoR), or EGFP-tagged Dnm2 (wild-type), CMT mutant K562E, or CNM mutant E560K. Confocal projection images of Dnm2 K562E (CMT)-expressing cultures show strongly reduced myelination as assessed by myelin basic protein (MBP) immunostaining 12 days after induction of myelination. Control, Dnm2 wild-type and E560K (CNM)-infected cultures display normal myelination. A comparable, extensive neuritic network was present in all conditions (immunostaining for neurofilaments; NF-160). (**B**) Quantification of MBP staining revealed significantly reduced myelination for cultures expressing Dnm2 CMT mutants (except for K562Δ) and for Dnm2 K44A. No significant alterations were found for CNM mutants R465W and E560K in comparison with controls (wild-type and pSicoR). Values represent means ± SD of three independent experiments: *$P < 0.05$, **$P < 0.01$, Student's *t*-test. Scale bars: 75 μm.

control or wild-type-overexpressing cultures, also without detectable neuronal defects (Fig. 4C). Expression of Dnm2 K44A and the CMT mutants G358R, G537C, K559Δ, K562E and L570H impaired myelination (Fig. 4D), but the effects were less prominent if compared with the corresponding experiments using heterozygous Dnm2$^{wt/0}$ dorsal root ganglia cultures (Fig. 2B). Again, the CNM mutants R465W and E560K showed no effects.

In complementary experiments, we ablated *Dnm2* specifically in Schwann cells using transgenic mice in which Cre expression is controlled by *Dhh* gene regulatory elements

Figure 3 CMT-causing Dnm2 mutants cause demyelination in heterozygous Dnm2$^{wt/0}$ dorsal root ganglia explant cultures. (**A**) Dorsal root ganglia explants dissected from Dnm2$^{wt/0}$ embryos were induced to myelinate for 12 days (uninfected culture at day of infection; *left*). Sister plates of myelinated cultures were infected on the 12th day of culture with lentivirus encoding GFP alone (pSicoR), EGFP-tagged Dnm2 (wild-type), CMT mutant K562E or CNM mutant E560K. Confocal projection images of Dnm2 K562E (CMT)-expressing cultures show aberrant myelin structures including signs of myelin swellings (arrows) and degradation (arrowheads), assessed by myelin basic protein (MBP) immunostaining 8 days after infection. The neuritic network (NF-160 immunostaining) was not detectably altered in all conditions. (**B**) MBP staining revealed significantly reduced MBP-fluorescence intensities for cultures expressing the Dnm2 CMT mutants G358R, K562E and for Dnm2 K44A. No significant alteration was found for CNM mutant E560K in comparison with controls (wild-type and pSicoR). Values represent means ± SD of three independent experiments: *$P < 0.05$, Student's *t*-test. Scale bars: 75 μm.

(Jaegle *et al.*, 2003). We first examined dorsal root ganglia cultures from DhhCre$^+$; Dnm2$^{wt/flox}$ embryos to evaluate if loss of one *Dnm2* allele in Schwann cells is sufficient to perturb myelination (Fig. 5A). Dorsal root ganglia cultures from this genotype myelinated normally, as did wild-type-overexpressing cultures. Myelination was impaired, however, by CMT mutants G358R, G537C, K559Δ, K562E, L570H and Dnm2 K44A (Fig. 5B). In contrast, the CNM mutants R465W and E560K, as well as the CMT mutant K562Δ had no significant effect. These results are strikingly similar to the data obtained with Dnm2$^{wt/0}$ dorsal root ganglia cultures (Fig. 2B). Thus, the reduced myelination observed in the latter experiments is most likely due to the reduced Dnm2 levels specifically in Schwann cells.
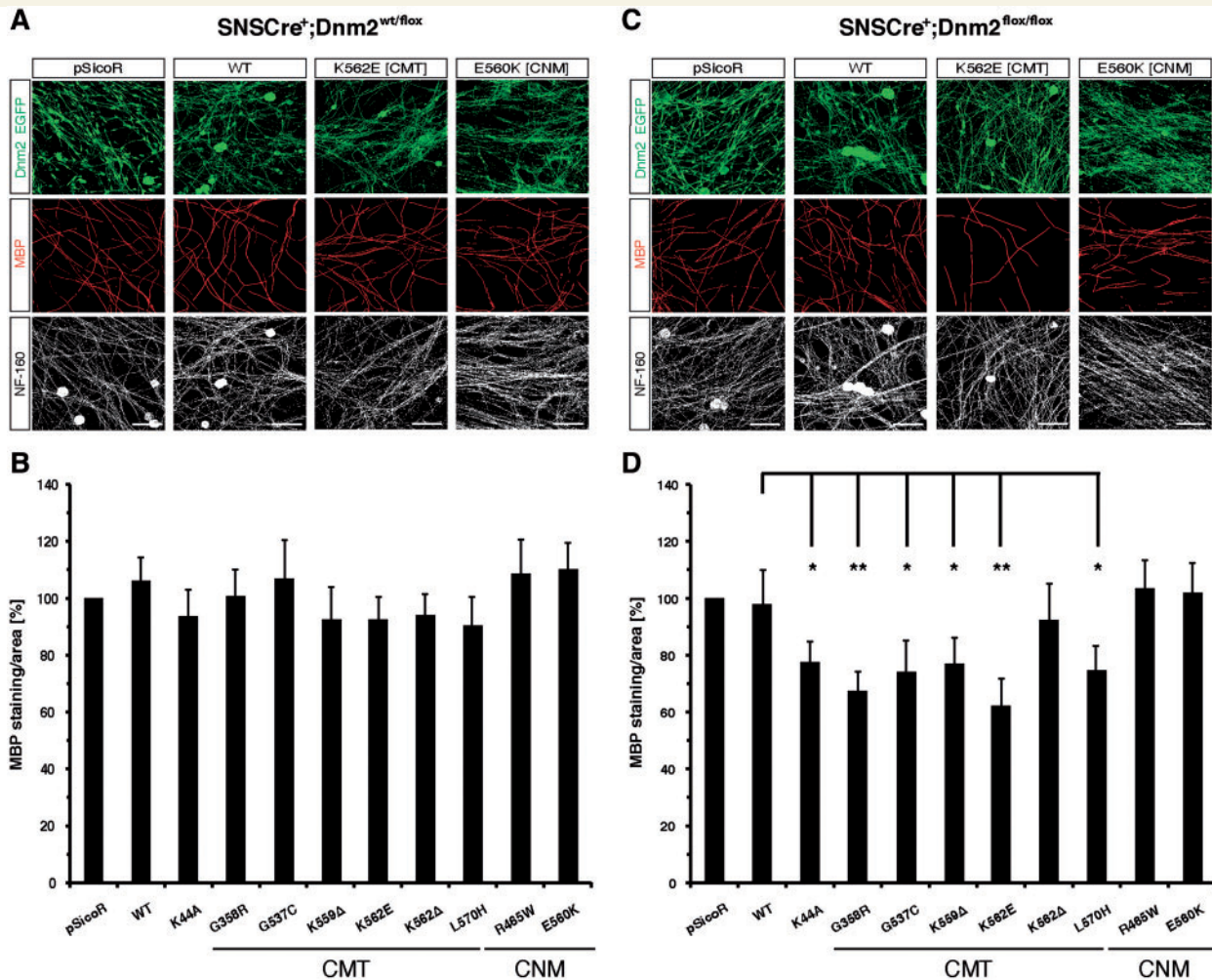
Figure 4 Dnm2 CMT mutants have a minor detrimental effect on myelination of dorsal root ganglia explants with specifically altered *Dnm2* gene dosage in sensory neurons. (**A** and **B**) Heterozygous ablation of *Dnm2* specifically in sensory neurons (SNSCre $^+$; Dnm2$^{wt/flox}$) revealed no significantly altered myelination [myelin basic protein (MBP) staining] in dorsal root ganglia explant cultures upon expression of Dnm2 CMT and CNM disease mutants compared with control-infected (pSicoR) and wild-type-infected settings. (**C**) In dorsal root ganglia explant cultures homozygously deleted for *Dnm2* in sensory neurons (SNSCre $^+$; Dnm2$^{flox/flox}$), myelination was indistinguishable between uninfected (not shown), control-infected and wild-type-transduced cultures. Expression of CMT mutant K562E impairs myelination, whereas CNM mutant E560K has no influence. Immunostaining for the neuritic network (NF-160) revealed no differences in all conditions. (**D**) MBP staining was decreased significantly in cultures expressing Dnm2 K44A and CMT mutants G358R, G537C, K559Δ, K562E and L570H, but not for CNM mutants R465W and E560K; and K562Δ (CMT). Quantified values represent means ± SD of three independent experiments: *$P < 0.05$, **$P < 0.01$, Student's t-test. Scale bars: 75 μm. WT = wild-type.

Next, we examined dorsal root ganglia cultures with complete *Dnm2* ablation in Schwann cells (DhhCre $^+$; Dnm2$^{flox/flox}$). Uninfected (data not shown) and control-infected dorsal root ganglia cultures of this genotype failed totally to myelinate (Fig. 5C and D). The defect could be rescued, however, by overexpression of Dnm2 wild-type. This finding is important since it shows that the loss of Dnm2 in Schwann cells had not damaged the cultures irreversibly. In contrast to Dnm2 wild-type, CMT mutants G358R, G537C, K559Δ, K562E, L570H and Dnm2 K44A were unable to rescue myelination (Fig. 5C and D). The CNM mutants R465W and E560K, however, rescued myelination analogously to Dnm2 wild-type protein. The CMT mutant K562Δ showed partial rescue activity. Interestingly, we found also that overexpression of

Dnm1 or Dnm3 was able to restore myelination in DhhCre $^+$; Dnm2$^{flox/flox}$ cultures (Supplementary Fig. 3). Thus, the missing molecular function(s) of Dnm2 in this experimental setting is shared by all three dynamin isoforms.

Taken together, we have shown that Dnm2 CMT—but not CNM-mutants have a destructive effect in a peripheral nerve disease model. Furthermore, Schwann cell-expressed Dnm2 is required for myelination, whereas Dnm2 expression by sensory neurons is dispensable. Schwann cell-specific ablation of *Dnm2* rendered the peripheral nerve model more sensitive to CMT mutants than analogous ablation, specifically in sensory neurons. In both cell types, the effect of CMT mutants is dependent on the endogenous *Dnm2* gene dosage.
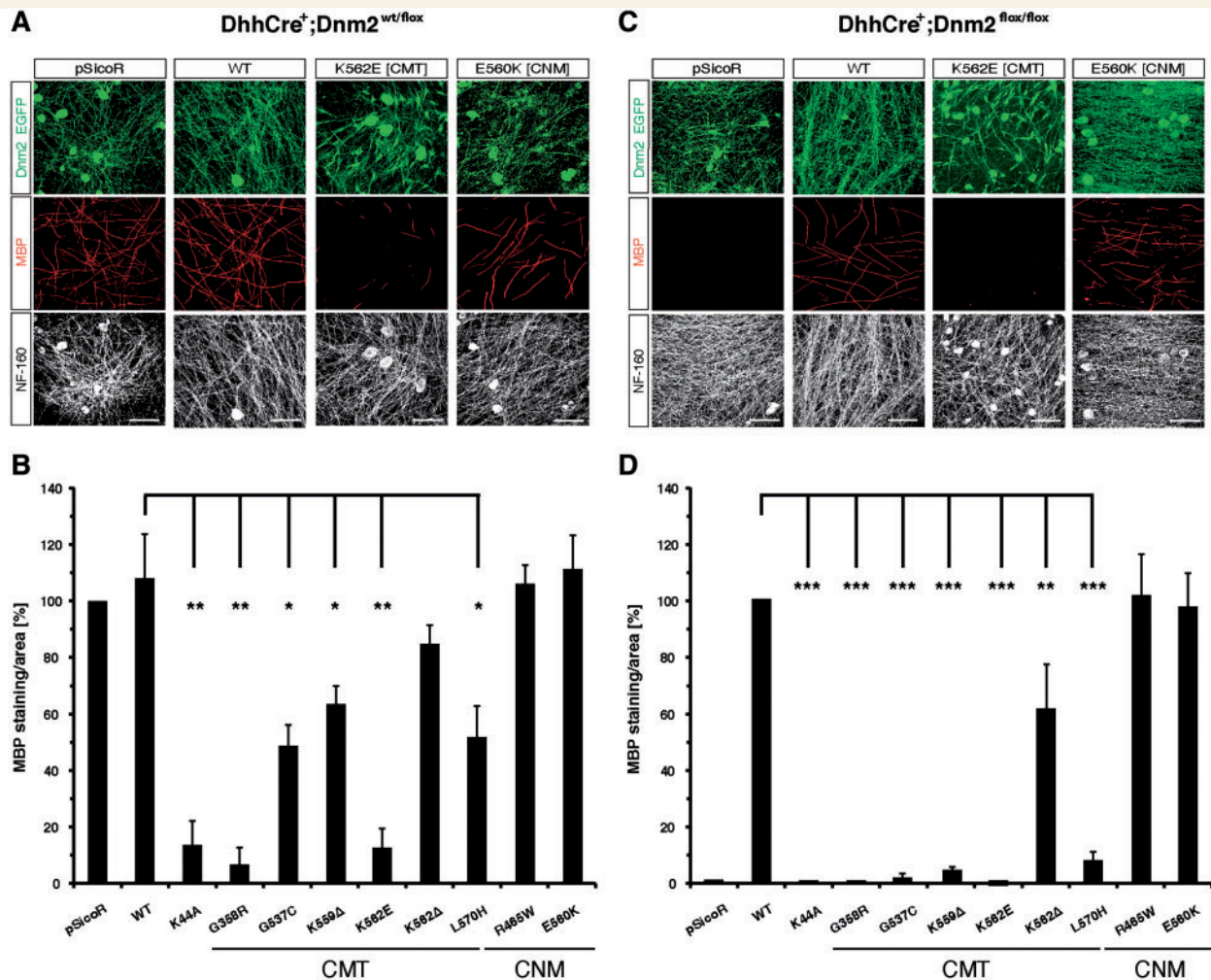
Figure 5 Schwann cells require Dnm2 for myelination and reduced endogenous *Dnm2* gene dosage in Schwann cells renders dorsal root ganglia cultures highly susceptible to harmful effects of CMT mutants. (**A**) Myelination [myelin basic protein (MBP) staining] of dorsal root ganglia explants with a DhhCre$^+$; Dnm2$^{wt/flox}$ background was reduced by expression of the Dnm2 CMT mutant K562E, but not by the CNM mutant E560K, compared with control (pSicoR) or WT-infected cultures. (**B**) MBP staining was significantly decreased in cultures expressing Dnm2 K44A and CMT mutants G358R, G537C, K559Δ, K562E and L570H. Dnm2 K562Δ (CMT) and CNM mutants R465W and E560K did not have a significant influence. (**C**) Complete ablation of *Dnm2* in Schwann cells (DhhCre$^+$; Dnm2$^{flox/flox}$ genotype) resulted in loss of myelination as revealed by myelin basic protein staining in pSicoR control-infected cultures. This effect was rescued by expression of Dnm2 WT and CNM mutant E560K, whereas the expression of the Dnm2 CMT mutant K562E was not able to rescue the defect. The neuritic network (NF-160 immunostaining) was not altered in all conditions. (**D**) Dnm2 K44A and CMT mutants G358R, G537C, K559Δ, K562E and L570H showed virtually no rescue capabilities, whereas expression of the CMT mutant K562Δ led to partial rescue. Expression of CNM mutants R465W or E560K was able to fully rescue the defect, comparable with WT expression. Data represent means ± SD of three independent experiments: *$P < 0.05$, **$P < 0.01$, ***$P < 0.001$, Student's *t*-test. Scale bars: 75 μm. WT = wild-type.

Inhibition of clathrin-mediated endocytosis by Dnm2 CMT-causing mutants

Dnm2 has a well-known critical function in endocytotic processes, and CMT and CNM mutants impaired clathrin-mediated endocytosis in various heterologous cell lines (Altschuler *et al*., 1998; Zuchner *et al*., 2005; Bitoun *et al*., 2009; Durieux *et al*., 2010). We hypothesized, partially based on our results with dorsal root

ganglia cultures, that the effects of the different mutations may be cell type-specific with regard to endocytosis. Thus, we investigated the consequences of mutant Dnm2 protein expression on endocytotic pathways in disease-relevant Schwann cells and differentiated mouse motor neuronal NSC-34 cells. To obtain definitive quantitative data, we established an uptake assay with labelled transferrin to measure clathrin-mediated endocytosis using fluorescence-activated flow cytometry. Alexa Fluor 647-labelled transferrin was measured in correlation to protein (EGFP) levels. This experimental set up allowed us to functionally characterize

the effects of disease-causing mutations on clathrin-mediated endocytosis compared with transgene expression levels (Supplementary Fig. 4A). We validated dynamin-dependent internalization of transferrin in our experimental system using dynasore, a potent inhibitor of large GTPases (Macia *et al.*, 2006). Dynasore-treated Schwann cells (rat Schwannoma cell line RT4) showed reduced transferrin uptake from 80 µM (25 ± 2.9%) to 120 µM (80 ± 4.9%) in a concentration-dependent manner compared with solvent-treated (ethanol) cells (Supplementary Fig. 4B). For the analysis of Dnm2 mutants, we first expressed disease-associated Dnm2 mutants in differentiated motor neurons (cell line NSC-34). Qualitative analyses by confocal microscopy revealed strongly reduced transferrin uptake by cells expressing the CMT mutant K562E, whereas the CNM mutant E560K had no detectable defect compared with the control and wild-type situation (Fig. 6A). We extended the analyses to groups of CMT and CNM mutants using quantitative flow cytometry (Fig. 6B). The CMT mutants G358R, G537C, K559Δ, K562E, K562Δ, L570H and Dnm2 K44A showed impaired clathrin-mediated endocytosis, whereas all 11 CNM mutants analysed in parallel did not alter transferrin uptake. Next, we carried out the same experiments in Schwann cells (RT4 cell line). Again, CMT mutants impaired transferrin uptake, with the exception of K562Δ (Fig. 6C; note that the same mutant had already shown a peculiar behaviour with effects ranging from 'weak to not significant' in dorsal root ganglia cultures). As in the motor neuron cell line, CNM mutants did not evoke detectable alterations of transferrin uptake in the Schwann cell line (Fig. 6C). Selected mutants were also tested qualitatively in rat primary Schwann cells using labelled transferrin and confocal microscopy. Dnm2 K44A and the CMT mutants G358R, G537C, K562E and L570H inhibited transferrin internalization. In contrast, the CNM mutant E560K showed no detectable effect (Supplementary Fig. 5). These results confirm the data obtained with RT4 cells.

Decreased cell surface levels of transferrin receptor may also contribute to reduced transferrin uptake. To investigate this issue, we transfected RT4 cells transiently with EGFP-tagged Dnm2 disease-associated mutants and examined the cells 24 h later by live cell immunostaining and qualitative confocal microscopy for transferrin receptor cell surface levels. Control, Dnm2 wild-type and CNM mutant E560K-transfected cells revealed a comparable punctuated cell surface transferrin receptor staining, whereas expression of the CMT mutant K562E increased this staining (Fig. 7A). We extended the analysis to additional CMT and clathrin-mediated endocytosis mutants and quantified transferrin receptor cell surface levels by flow cytometry. Overall, none of the tested mutants reduced the transferrin receptor surface levels. The CMT mutants G358R, G537C, K562E and Dnm2 K44A even induced a significant increase of relative transferrin receptor cell surface levels compared with Dnm2 wild-type transfected cells (Fig. 7B). We interpreted these results in that elevated transferrin receptor cell surface levels are due to receptor trapping on the surface by impaired endocytosis. Alternatively, transport of membrane proteins to the cell surface could be affected in general. To examine this possibility, we infected rat primary Schwann cells with lentiviral vectors to achieve expression of mutants and controls. After 4 days, the cells were pulse-labelled

with ^{35}S-*L*-methionine/*L*-cysteine for 20 min followed by cell surface biotinylation and purification of biotinylated proteins. ^{35}S-labelled proteins (input) and cell surface-biotinylated ^{35}S-labelled proteins (beads) were analysed by sodium dodecyl sulphate–polyacrylamide gel electrophoresis (Supplementary Fig. 6A), detected by autoradiography and quantified. The amounts of labelled cell surface proteins in relation to totally labelled proteins were determined (Supplementary Fig. 6B). We found no significant differences between cells that expressed Dnm2 K44A, CMT mutants (G358R, K562E) or the CNM mutant E560K compared with control or wild-type overexpressing cells indicating no overt alteration of transport of the newly synthesized proteins to the plasma membrane. In contrast and as expected, brefeldin A and dynasore-treated cells reduced trafficking of newly synthesized proteins to the plasma membrane compared with controls (Supplementary Fig. 6C and D).

We conclude that in Schwann cells, CMT but not CNM mutants inhibit clathrin-mediated endocytosis without affecting the transport of cell surface proteins to the plasma membrane. Furthermore, impaired transferrin uptake appears not to be the result of decreased transferrin receptor surface levels, but the consequence of direct inhibition of clathrin-mediated endocytosis as shown before for Dnm2 K44A (Altschuler *et al.*, 1998).

CMT-associated Dnm2 mutations alter membrane receptor surface level of proteins essential for Schwann cell biology

Schwann cells require precise amounts of cell surface receptors for correct migration, myelination, survival and interaction with the accompanying axon (Pereira *et al.*, 2012). Such processes are likely disturbed by Dnm2 mutations in dominant-intermediate CMT subtype B. Thus, we hypothesized that besides the transferrin receptor, other surface proteins might be affected by impaired clathrin-mediated endocytosis due to Dnm2 mutations. We therefore first determined the rat primary Schwann cell surface glycoproteome with an antibody-independent, mass spectrometry-based cell-surface capturing approach (Wollscheid *et al.*, 2009; Hofmann *et al.*, 2010). In total, 211 glycoproteins of the rat primary Schwann cell surface proteome were identified (Supplementary Fig. 7A and Supplementary Table 3). Out of these, integrin β$_1$ (ITB1_RAT, CD29) and the receptor tyrosine-protein kinase ErbB-2 (ERBB2_RAT, CD340) were further analysed. We selected integrin β$_1$ as the first potentially Dnm2 mutant-affected protein, since α$_6$β$_1$-integrin is internalized via a dynamin-dependent pathway in colonic epithelial cells (Vassilieva *et al.*, 2008), and Schwann cell-expressed integrin β$_1$ is critical for peripheral nerve function (Berti *et al.*, 2006). Rat primary Schwann cells were infected with lentiviral vectors encoding EGFP (pSicoR), Dnm2 wild-type or the CMT mutant K562E, followed 4 days later by cell surface biotinylation and purification of biotinylated plasma membrane proteins. We found that surface integrin β$_1$ levels were significantly increased on K562E expressing rat primary Schwann cells compared with wild-type over-expressing cells or controls (Fig. 7C). Parallel staining with Cy3-coupled streptavidin of
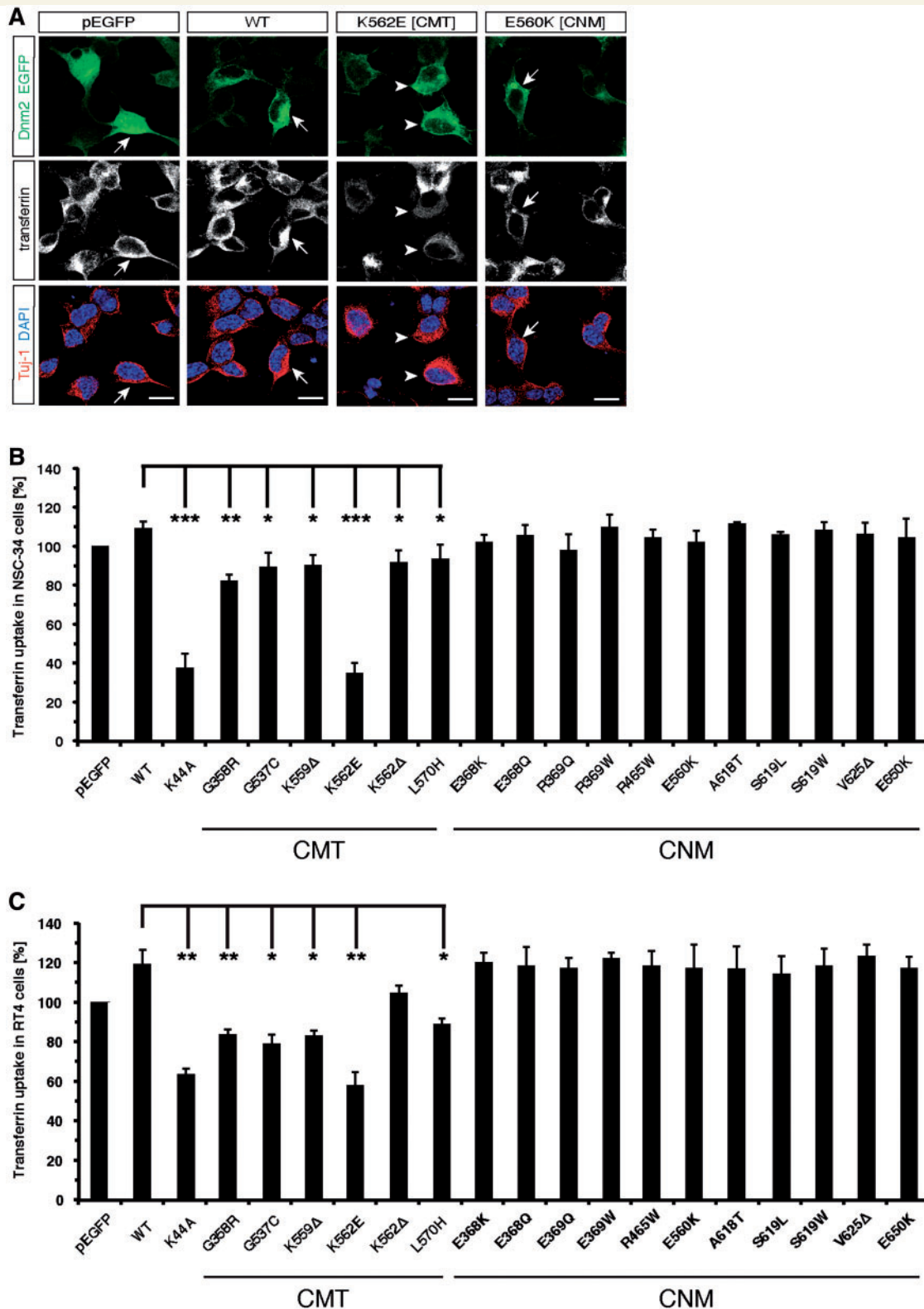
Figure 6 Dnm2 CMT mutants impair clathrin-mediated endocytosis in motor neurons and Schwann cells, whereas CNM mutants have no effect. (**A**) NSC-34 motor neurons were transfected in proliferative conditions to express EGFP, EGFP-tagged wild-type, or mutant Dnm2 proteins. After 24 h, cells were differentiated for an additional 72 h. After serum starvation, transferrin uptake (20 μg/ml Alexa Fluor 555-labelled transferrin) was allowed (15 min), followed by immunostaining for the neuronal marker Tuj-1. Confocal images illustrate an inhibition of transferrin uptake for cells expressing Dnm2 K562E (CMT) (arrowheads) compared with EGFP control-transfected and EGFP-Dnm2 wild-type expressing cells (arrows). Expression of the CNM mutant E560K does not inhibit transferrin uptake (arrow). Scale bars: 15 μm. (**B**) Quantification by fluorescence-activated flow cytometry revealed impaired transferrin uptake by Dnm2 mutant K44A and

untreated and detergent-treated cells expressing EGFP-tagged Dnm2 wild-type validated the experimental setting (Supplementary Fig. 7B). Next, we examined ErbB2, an essential regulator of Schwann cell–axon interactions (Newbern and Birchmeier, 2010), which is internalized in a clathrin-dependent manner (Michailov *et al.*, 2004; Sorkin *et al.*, 2008). Using the same basic experimental set up as for the integrin β_1 studies, the timing of ErbB2 internalization after stimulation with NRG-1 type III was determined (Supplementary Fig. 7C). A total of 1 h of stimulation was established to be optimal for our purpose. Under these conditions, the levels of ErbB2 on the cell surface of Dnm2 K44A or CMT mutant K562E expressing cells were significantly higher than on control- or wild-type over-expressing cells (Fig. 7D). These results demonstrate an important role for Dnm2-dependent receptor internalization in Schwann cells that is altered by the CMT mutant K562E.

Clathrin-mediated endocytosis is essential for myelination of dorsal root ganglia cultures

Our data indicated an inhibition of clathrin-mediated endocytosis by CMT mutants. Thus, we asked whether altered endocytosis is sufficient to explain the impairment of myelination in our peripheral nerve model (dorsal root ganglia cultures). We decided to approach this question by knocking down the expression of the specific clathrin adaptor at the plasma membrane, AP-2 subunit μ2 (AP-2), to inhibit clathrin-mediated endocytosis (Motley *et al.*, 2003). For this purpose, we developed two short hairpin RNAs targeting AP-2. Both of them, after delivery into rat primary Schwann cells with lentiviral vectors, resulted in significant decrease of AP-2 protein levels 4 days post-infection (Fig. 8A). As expected, AP-2 knock-down resulted in severe inhibition of transferrin uptake as qualitatively analysed by confocal microscopy (data not shown). These results were confirmed and quantified by flow cytometry in RT4 cells (Fig. 8B). Cell surface biotinylation of pulse ^{35}S-*L*-methionine/*L*-cysteine-labelled rat primary Schwann cells revealed that AP-2 knock-down does not influence transport of cell surface proteins to the plasma membrane (Fig. 8C and D).

We used the established AP-2 short hairpin RNAs in dorsal root ganglia cultures to test for effects of AP-2 knock-down on myelination. Dorsal root ganglia cultures infected with lentiviral vectors encoding the AP-2 targeting short hairpin RNA 747 survived well, but failed to myelinate, whereas control DsRed2 short hairpin RNA-infected cultures myelinated normally (Fig. 8E). Cultures in which the more efficient AP-2 targeting short hairpin RNA 748 (Fig. 8A) was used did not survive, indicating that a too strong reduction of clathrin-mediated endocytosis is not tolerated in this

experimental setting (data not shown). This interpretation is supported by comparable experiments employing short hairpin RNAs against clathrin, in which the cultures also did not survive (data not shown). We conclude that proper functional clathrin-mediated endocytosis is required for myelination in our model. These findings are consistent with the observation that CMT-associated Dnm2 mutants that affect clathrin-mediated endocytosis in cultured neurons and Schwann cells are also deleterious in dorsal root ganglia myelination cultures.

Discussion

Dnm2 is a ubiquitously expressed protein with various cellular functions. Despite these pleiotropic roles, *DNM2* mutations are associated with distinct diseases and affect a limited number of cell types such as Schwann cells and/or neurons of the PNS in dominant-intermediate CMT subtype B, or muscle cells in autosomal dominant CNM. In this study, we compared the effects of CMT and CNM mutants in a PNS model and in cell cultures of PNS-derived cells to elucidate disease mechanisms in dominant-intermediate CMT subtype B and to address the intriguing question of why CNM mutants do not affect the PNS.

We established a disease-related peripheral nerve model using tissue from Dnm2$^{wt/0}$ transgenic mice and showed that expression of CMT mutants had strikingly harmful effects, whereas expression of CNM mutants was without consequences. These results validated the model for additional investigations. Importantly, further analyses discovered that changes in endogenous *Dnm2* gene dosage have a profound influence. In particular, expression of CMT mutants on a Dnm2$^{wt/wt}$ background did not cause defects demonstrating that the endogenous gene dosage modulates the consequences of CMT mutants. Further analyses using cell type-specific modulation of endogenous gene dosage revealed that such alterations in Schwann cells had a more pronounced effect compared with sensory neurons. However, the system was sensitive to such changes in both cell types with respect to the effects of CMT mutants. Complete ablation of *Dnm2* in Schwann cells caused a total loss of myelin formation demonstrating that Schwann cell Dnm2 function is indispensable for myelination. Re-expression of Dnm2 rescued the phenotype, while CMT mutants could not. Expression of CNM mutants, however, was able to rescue myelination efficiently indicating that CMT mutant proteins have lost an essential PNS function that CNM mutants can still provide. Interestingly, expression of Dnm1 or Dnm3 was also able to rescue myelination in this experimental setting indicating that the critical Dnm2 function is shared by the dynamin isoforms. The cellular and molecular mechanisms underlying the observed, at least partially cell type-specific, gene dosage sensitivities remain

Figure 6 Continued

by all tested CMT mutants compared with the wild-type overexpression setting. CNM mutants did not alter transferrin uptake. (**C**) RT4 Schwann cells were transfected to express the proteins indicated and 24 h later, transferrin uptake was analysed as described above using flow cytometry. Transferrin uptake was reduced by the expression of Dnm2 K44A and CMT mutants G358R, G537C, 551Δ3, K559Δ, K562E and L570H. Dnm2 K562Δ (CMT) and all CNM mutants tested had no significant effect. Values represent means ± SD of three independent experiments: *$P < 0.05$, **$P < 0.01$, ***$P < 0.001$, Student's *t*-test. WT = wild-type.
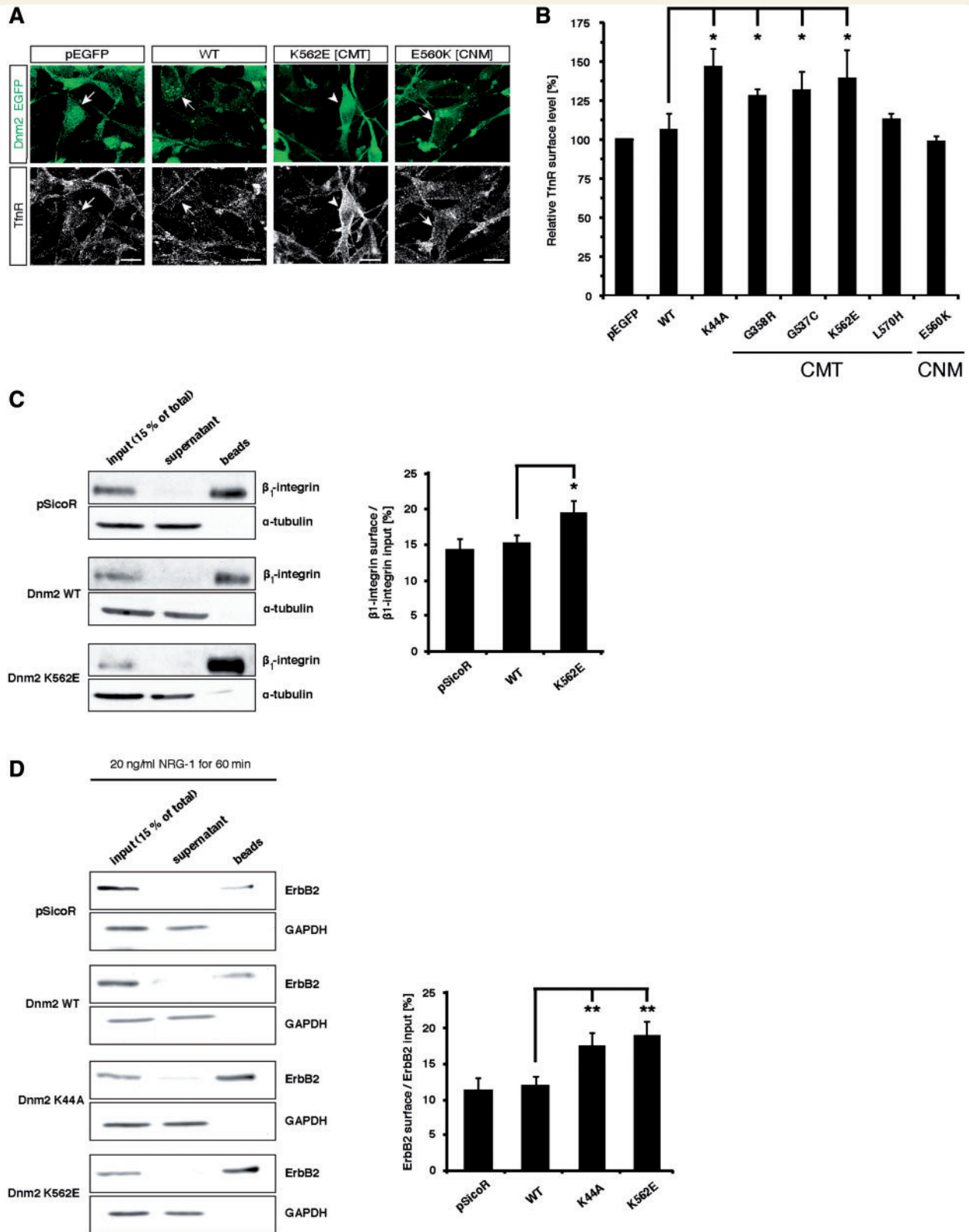
Figure 7 Transferrin receptor-, ErbB2- and integrin β_1 cell surface levels are elevated on Schwann cells expressing Dnm2 CMT mutants. (**A**) RT4 Schwann cells were transfected with EGFP-tagged Dnm2, Dnm2 mutants, or control constructs followed by live cell transferrin receptor immunostaining 24 h later. Confocal images of control (pEGFP), Dnm2 wild-type (WT) and CNM mutant E560K-expressing cells show a punctuate transferrin receptor cell surface pattern (arrows). Expression of Dnm2 CMT mutant K562E results in an increased cell surface level of transferrin receptor (arrowhead). Scale bars: 15 μm. (**B**) Transferrin receptor cell surface amounts were quantified by flow cytometry on cells with mid-range expression of exogenous proteins (Supplementary Fig. 4). Transferrin receptor cell surface levels were

to be elucidated. We speculate, however, that endogenous expression levels of the classical dynamin family members in the presence of Dnm2 mutants are likely to be a key issue.

Previous studies have suggested, based on analyses in fibroblasts, that both CMT (K562E) and CNM (R465W, V625Δ, E650K) mutants impair clathrin-mediated endocytosis (Bitoun *et al.*, 2009; Durieux *et al.*, 2010). We extended these studies and found that in HeLa cells, none of the tested CNM mutants (E368K, E368Q, E369Q, E369W, R465W, E560K, A618T, S619L, S619W, V625Δ and E650K), including the mutants tested in fibroblasts previously, inhibited clathrin-mediated endocytosis even if highly expressed (data not shown). In contrast, some CMT mutants (G358R, G537C, K559Δ and K562E) significantly inhibited clathrin-mediated endocytosis while others (D555_E557Δ, K562Δ and L570H) did not (data not shown). The variability of these data, obtained using heterologous, non-disease-relevant cell types, indicates the importance of examining the effects of Dnm2 mutants in appropriate cellular settings, since these mutants appear to affect clathrin-mediated endocytosis differently, depending on the cell type used for analysis. Thus, we focused our experiments on cell lines and primary cells that originate from CMT-related tissue. As in HeLa cells, we found that CMT mutants G358R, G537C, K559Δ, K562E and additionally L570H impair clathrin-mediated endocytosis in Schwann cells and in motor neurons, whereas CNM mutants do not show a detectable effect. Interestingly, the CMT mutant K562Δ had no significant impact on clathrin-mediated endocytosis in Schwann cells and only a minor effect in motor neurons suggesting that this mutant has different characteristics compared with the bulk of the CMT mutants. These data are consistent with the divergent effects of the K562Δ mutant compared with the other CMT mutants in our peripheral nerve model, and warrant further investigations into a mutant-specific disease mechanism. However, we found that CMT and CNM mutants have distinct consequences on clathrin-mediated endocytosis in cells originating from the PNS; CMT mutants affect clathrin-mediated endocytosis in CMT-relevant cell types, whereas CNM mutants have no effect. The CMT mutant-specific effect on clathrin-mediated endocytosis in cells derived from the PNS are coherent with the fact that CMT mutants lead to dominant-intermediate CMT subtype B and indicate th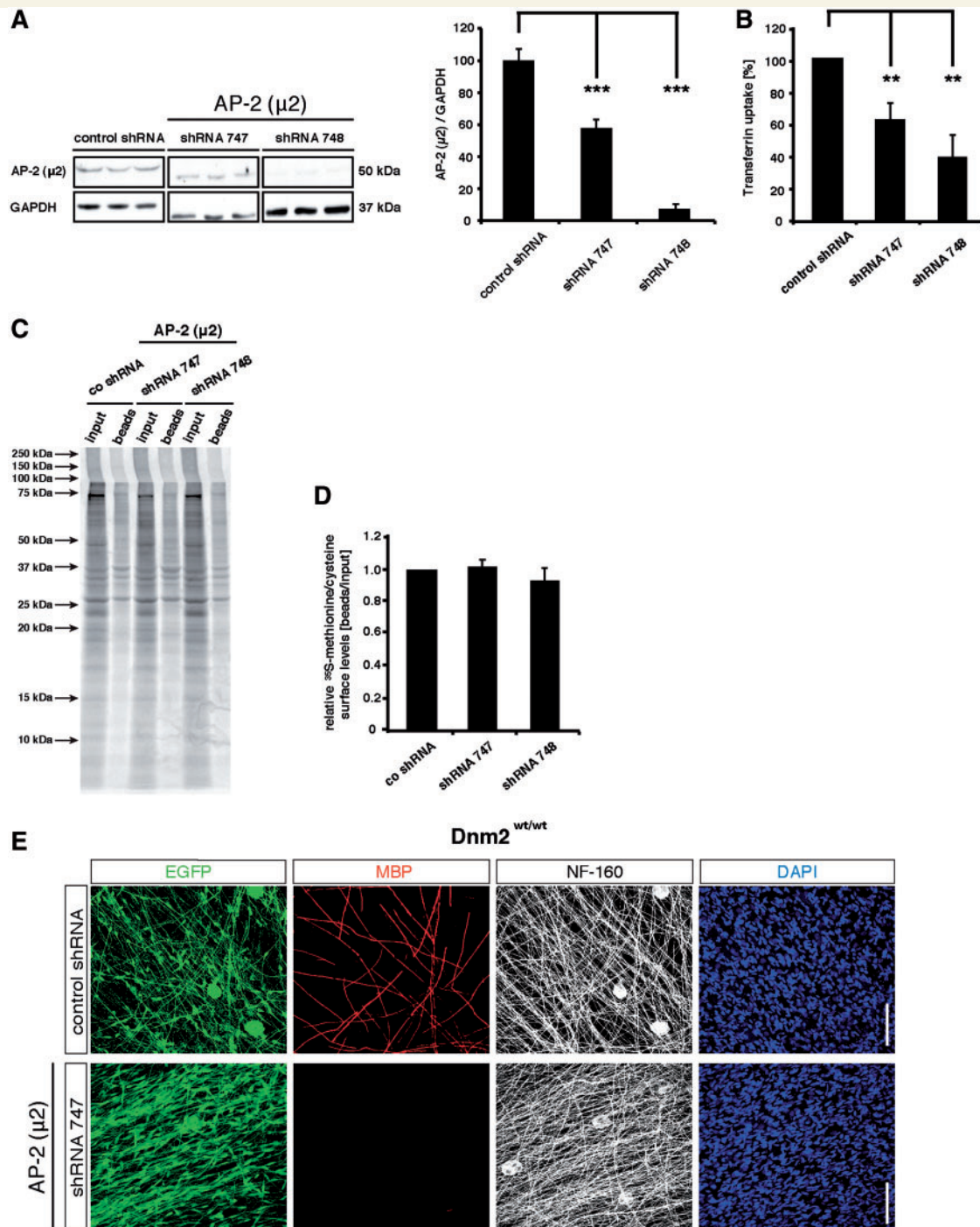at altered clathrin-mediated endocytosis contributes to the dominant-intermediate CMT subtype B disease mechanism. In further support of this hypothesis, we demonstrated that short hairpin RNA-mediated knock-down of the plasma membrane-specific clathrin adaptor AP-2 is sufficient to inhibit myelination in dorsal root ganglia cultures comparable with the effects caused by CMT mutants. We conclude that clathrin-mediated endocytosis is critical for proper peripheral nerve myelination and defects in this cellular function, caused by CMT mutants, are likely to contribute to the observed PNS pathophysiology in dominant-intermediate CMT subtype B.

We have focused our studies on dominant-intermediate CMT subtype B and the PNS. With regard to CNM mutants, our data indicate that they do not cause CMT, since they do not affect clathrin-mediated endocytosis in cells of the PNS. The findings that CNM mutants, but not CMT mutants, are able to rescue the phenotype of Dnm2 loss in Schwann cells in our peripheral nerve model lend further support to this notion. In contrast, CNM mutants have been shown to alter clathrin-mediated endocytosis in fibroblast, whereas we have not found such effects in HeLa cells. These divergent results may be explained by the specific cell biology of epithelial-like HeLa cells that are more closely related to polarized cells of the PNS including myelinating Schwann cells (Ozcelik *et al.*, 2010) than fibroblasts and myoblasts. Taken together, it is conceivable but speculative that CNM mutants might also affect clathrin-mediated endocytosis in skeletal muscle cells by a combined mutant- and cell type-specific mechanism that contributes to the disease. However, other mechanisms are also possible (Kenniston *et al.*, 2010; Wang *et al.*, 2010) and thus, the question of how CNM mutants cause a specific disease in skeletal muscles remains open.

The elucidation of disease mechanisms is of considerable value to learn more about the basic biology of cells and tissues, but such studies also ultimately aim at providing suitable targets for therapeutic strategies. In this respect, clathrin-mediated endocytosis is a rather pleiotropic pathway and difficult to target without the expectation of major side effects. Though, specific plasma membrane proteins with critical PNS functions are likely to be affected and to contribute to the disease development. As a prerequisite to identify such candidates, we employed the mass spectrometry-based cell surface capturing strategy to generate a snapshot

Figure 7 Continued

found to be significantly increased by the expression of Dnm2 K44A and Dnm2 CMT mutants G358R, G537C and K562E compared with cells expressing Dnm2 wild-type. Values represent means ± SD of three independent experiments: *$P < 0.05$, Student's *t*-test. (**C**) To examine cell surface levels of β_1-integrin, rat primary Schwann cells were control-infected (pSicoR), or infected with lentivirus encoding Dnm2 wild-type or K562E (CMT) for 96 h, followed by surface biotinylation and purification of biotinylated proteins (beads). Western blot analysis revealed elevated integrin β_1 cell surface levels for cells expressing Dnm2 CMT mutant K562E compared with control and wild-type infected conditions. α-Tubulin served as negative control for the purification of surface proteins. The graph represents values of cell surface integrin β_1 levels (beads) in relation to total (input) amounts as means ± SD of three independent experiments: *$P < 0.05$, Student's *t*-test. (**D**) To examine clathrin-mediated endocytosis-dependent internalization of ErbB2, rat primary Schwann cells were either control-infected (pSicoR), or infected with lentivirus encoding Dnm2 WT, K44A, or K562E (CMT) and incubated for 96 h. Cells were serum-starved for 4 h and stimulated with 20 ng/ml NRG-1 type III for 1 h, followed by surface biotinylation. Dnm2 K44A and K562E (CMT) decreased ErbB2 internalization significantly compared with Dnm2 WT as indicated by increased cell surface levels of ErbB2. GAPDH served as negative control for surface biotinylation. Quantitation represents means ± SD of three independent experiments: **$P < 0.01$, Student's *t*-test.

Figure 8 Expression knock-down of the plasma membrane-specific clathrin adaptor protein AP-2 impairs clathrin-mediated endocytosis in Schwann cells and prevents myelination of dorsal root ganglia cultures. (**A**) Rat primary Schwann cells were infected with lentiviral vectors (Ubc-TurboGFP) expressing AP-2 (μ2)-targeting short hairpin RNA 747 and short hairpin RNA 748 that result in AP-2 (μ2) protein knock-down with different efficiencies in comparison with control-infected (short hairpin RNA targeting DsRed2) cells [4 days post-infection (dpi)] as shown by immunoblotting. GAPDH served as loading control. Graph shows relative AP-2 protein expression levels (means $\pm$ SD of three independent infections: ***$P < 0.001$, Student's t-test). (**B**) Transferrin uptake was inhibited in RT4 Schwann cells expressing short hairpin RNAs against AP-2. On completing 4 days after transfection with short hairpin RNA expression constructs, also expressing EGFP under a separate promoter (Ubc-TurboGFP), cells were serum-starved and incubated with Alexa Fluor 647-labelled transferrin. Quantification by flow cytometry showed that transferrin uptake was significantly reduced for both short hairpin RNAs targeting AP-2 compared with control short hairpin RNA. Values represent means $\pm$ SD of three independent experiments: **$P < 0.01$, Student's t-test. (**C** and **D**) Rat primary Schwann cells infected with lentiviral vectors (Ubc-TurboGFP) expressing AP-2 (μ2)-targeting short hairpin RNA 747 and short hairpin RNA 748 were pulse labelled with ^{35}S-L-methionine/L-cysteine for 20 min, 4 days post-infection followed by surface biotinylation. Purified biotinylated surface proteins (beads) and total labelled proteins (input) were analysed by sodium

view of the rat primary Schwann cell surface glycoproteome. We detected 211 different cell surface exposed *N*-glycoproteins and database-assisted analysis revealed that 43 of these proteins have been previously linked to Dnm2- and/or clathrin-dependent endocytosis. We confirmed this link biochemically for integrin β_1 and ErbB2. Given their importance in PNS biology, both of these proteins might be involved in the pathogenesis of dominant-intermediate CMT subtype B but other proteins may also contribute. Together, our surface glycoproteome analysis on rat primary Schwann cells provides the mass spectrometry coordinates of selected *N*-glycopeptides, which can be used for the development of targeted assays applied in directed mass spectrometry-based approaches (e.g. selected reaction monitoring) (Anderson *et al.*, 2006; Lange *et al.*, 2008) for the quantification of cell surface exposed proteins in tissue and cells from appropriate animal models and patient material.

In summary, we introduce a peripheral nerve disease model that is particularly sensitive to destructive effects of CMT- but not of CNM-associated mutants. We demonstrate that these effects correlate with defects in clathrin-mediated endocytosis, which are caused specifically by CMT mutants in PNS-derived cells. CNM-associated mutants fail to have such effects providing a likely explanation for the tissue-specific phenotypes caused by CMT and CNM mutants. Our findings that myelination is sensitive to the expression of CMT-associated Dnm2 mutants, together with the dependence of myelination on Dnm2 and clathrin-mediated endocytosis function, indicate strongly that clathrin-mediated endocytosis is a critically affected pathway in dominant-intermediate CMT subtype B.

Acknowledgements

Funding

Supplementary material

Supplementary material is available at *Brain* online.

References

Agarwal N, Offermanns S, Kuner R. Conditional gene deletion in primary nociceptive neurons of trigeminal ganglia and dorsal root ganglia. Genesis 2004; 38: 122–9.

Altschuler Y, Barbas SM, Terlecky LJ, Tang K, Hardy S, Mostov KE, et al. Redundant and distinct functions for dynamin-1 and dynamin-2 isoforms. J Cell Biol 1998; 143: 1871–81.

Anderson L, Hunter CL. Quantitative mass spectrometric multiple reaction monitoring assays for major plasma proteins. Mol Cell Proteomics 2006; 5: 573–88.

Berti C, Nodari A, Wrabetz L, Feltri ML. Role of integrins in peripheral nerves and hereditary neuropathies. Neuromolecular Med 2006; 8: 191–204.

Bitoun M, Durieux AC, Prudhon B, Bevilacqua JA, Herledan A, Sakanyan V, et al. Dynamin 2 mutations associated with human diseases impair clathrin-mediated receptor endocytosis. Hum Mutat 2009; 30: 1419–27.

Claeys KG, Zuchner S, Kennerson M, Berciano J, Garcia A, Verhoeven K, et al. Phenotypic spectrum of dynamin 2 mutations in Charcot-Marie-Tooth neuropathy. Brain 2009; 132: 1741–52.

Durieux AC, Prudhon B, Guicheney P, Bitoun M. Dynamin 2 and human diseases. J Mol Med 2010; 88: 339–50.

Durieux AC, Vignaud A, Prudhon B, Viou MT, Beuvin M, Vassilopoulos S, et al. A centronuclear myopathy-dynamin 2 mutation impairs skeletal muscle structure and function in mice. Hum Mol Genet 2010; 19: 4820–36.

Dyck PJ, Chance P, Lebo R, Carney JA. Hereditary motor and sensory neuropathies. In: Dyck PJ, Thomas PK, Griffin JW, Low PA, Poduslo JF, editors. Peripheral neuropathy. Philadelphia: W.B. Saunders Company; 1993. p. 1094–136.

Ferguson SM, Brasnjo G, Hayashi M, Wolfel M, Collesi C, Giovedi S, et al. A selective activity-dependent requirement for dynamin 1 in synaptic vesicle endocytosis. Science 2007; 316: 570–4.

Ferguson SM, Raimondi A, Paradise S, Shen H, Mesaki K, Ferguson A, et al. Coordinated actions of actin and BAR proteins upstream of dynamin at endocytic clathrin-coated pits. Developmental cell 2009; 17: 811–22.

Fischer D, Herasse M, Bitoun M, Barragan-Campos HM, Chiras J, Laforet P, et al. Characterization of the muscle involvement in dynamin 2-related centronuclear myopathy. Brain 2006; 129: 1463–9.

Heymann JA, Hinshaw JE. Dynamins at a glance. J Cell Sci 2009; 122: 3427–31.

Hofmann A, Gerrits B, Schmidt A, Bock T, Bausch-Fluck D, Aebersold R, et al. Proteomic cell surface phenotyping of differentiating acute myeloid leukemia cells. Blood 2010; 116: e26–34.

Jaegle M, Ghazvini M, Mandemakers W, Piirsoo M, Driegen S, Levavasseur F, et al. The POU proteins Brn-2 and Oct-6 share important functions in Schwann cell development. Genes Dev 2003; 17: 1380–91.

Figure 8 Continued

dodecyl sulphate–polyacrylamide gel elctrophoresis and subsequent autoradiography. Quantifications revealed no impairment in transport of newly synthesized proteins to the plasma membrane relative to the total of the labelled proteins. Values represent means $\pm$ SD of three independent experiments. (**E**) Myelination was inhibited by knock-down of AP-2. Dnm2$^{wt/wt}$ dorsal root ganglia explants were infected with 5×10^8 TU/ml of lentivirus (Ubc-TurboGFP) encoding short hairpin RNA 747 targeting AP-2 and a control short hairpin RNA-expressing virus. Cultures were analysed 12 days after induction of myelination. Control-infected dorsal root ganglia explants myelinated normally as assessed by myelin basic protein (MBP) staining, whereas reduction of AP-2 protein levels resulted in no detectable myelination. The neuritic network (NF-160 staining) and total cell number (DAPI staining) were not affected. Scale bar: 75 µm.

Jain E, Bairoch A, Duvaud S, Phan I, Redaschi N, Suzek BE, et al. Infrastructure for the life sciences: design and implementation of the UniProt website. BMC Bioinformatics 2009; 10: 136.

Keller A, Nesvizhskii AI, Kolker E, Aebersold R. Empirical statistical model to estimate the accuracy of peptide identifications made by MS/MS and database search. Anal Chem 2002; 74: 5383–92.

Keller LC, Romijn EP, Zamora I, Yates JR 3rd, Marshall WF. Proteomic analysis of isolated chlamydomonas centrioles reveals orthologs of ciliary-disease genes. Curr Biol 2005; 15: 1090–8.

Kenniston JA, Lemmon MA. Dynamin GTPase regulation is altered by PH domain mutations found in centronuclear myopathy patients. EMBO J 2010; 29: 3054–67.

Lange V, Malmstrom JA, Didion J, King NL, Johansson BP, Schafer J, et al. Targeted quantitative analysis of Streptococcus pyogenes virulence factors by multiple reaction monitoring. Mol Cell Proteomics 2008; 7: 1489–500.

Liu YW, Surka MC, Schroeter T, Lukiyanchuk V, Schmid SL. Isoform and splice-variant specific functions of dynamin-2 revealed by analysis of conditional knock-out cells. Mol Biol Cell 2008; 19: 5347–59.

Macia E, Ehrlich M, Massol R, Boucrot E, Brunner C, Kirchhausen T. Dynasore, a cell-permeable inhibitor of dynamin. Developmental cell 2006; 10: 839–50.

Mi H, Lazareva-Ulitsky B, Loo R, Kejariwal A, Vandergriff J, Rabkin S, et al. The PANTHER database of protein families, subfamilies, functions and pathways. Nucleic Acids Res 2005; 33: D284–8.

Michailov GV, Sereda MW, Brinkmann BG, Fischer TM, Haug B, Birchmeier C, et al. Axonal neuregulin-1 regulates myelin sheath thickness. Science 2004; 304: 700–3.

Motley A, Bright NA, Seaman MN, Robinson MS. Clathrin-mediated endocytosis in AP-2-depleted cells. J Cell Biol 2003; 162: 909–18.

Nesvizhskii AI, Keller A, Kolker E, Aebersold R. A statistical model for identifying proteins by tandem mass spectrometry. Anal Chem 2003; 75: 4646–58.

Newbern J, Birchmeier C. Nrg1/ErbB signaling networks in Schwann cell development and myelinatio. Semin Cell Dev Biol 2010; 21: 922–28.

Nicholson G, Myers S. Intermediate forms of Charcot-Marie-Tooth neuropathy: a review. Neuromolecular Med 2006; 8: 123–30.

Ozcelik M, Cotter L, Jacob C, Pereira JA, Relvas JB, Suter U, et al. Pals1 is a major regulator of the epithelial-like polarization and the extension of the myelin sheath in peripheral nerves. J Neurosci 2010; 30: 4120–31.

Pedrioli PG, Eng JK, Hubley R, Vogelzang M, Deutsch EW, Raught B, et al. A common open representation of mass spectrometry data and its application to proteomics research. Nat Biotechnol 2004; 22: 1459–66.

Pereira JA, Lebrun-Julien F, Suter U. Molecular mechanisms regulating myelination in the peripheral nervous system. Trends Neurosci 2012; 35: 123–34.

Praefcke GJ, McMahon HT. The dynamin superfamily: universal membrane tubulation and fission molecules? Nat Rev Mol Cell Biol 2004; 5: 133–47.

Ramachandran R, Surka M, Chappie JS, Fowler DM, Foss TR, Song BD, Schmid SL. The dynamin middle domain is critical for tetramerization and higher-order self-assembly. EMBO J 2007; 26: 559–66.

Scherer SS, Wrabetz L. Molecular mechanisms of inherited demyelinating neuropathies. Glia 2008; 56: 1578–89.

Skre H. Genetic and clinical aspects of Charcot-Marie-Tooth's disease. Clin Genet 1974; 6: 98–118.

Sorkin A, Goh LK. Endocytosis and intracellular trafficking of ErbBs. Exp Cell Res 2008; 314: 3093–106.

Suter U, Scherer SS. Disease mechanisms in inherited neuropathies. Nat Rev Neurosci 2003; 4: 714–26.

Stendel C, Roos A, Kleine H, Arnaud E, Ozcelik M, Sidiropoulos PN, et al. SH3TC2, a protein mutant in Charcot-Marie-Tooth neuropathy, links peripheral nerve myelination to endosomal recycling. Brain 2010; 133: 2462–74.

Tanabe K, Takei K. Dynamic instability of microtubules requires dynamin 2 and is impaired in a Charcot-Marie-Tooth mutant. J Cell Biol 2009; 185: 939–48.

Thomas PD, Kejariwal A, Campbell MJ, Mi H, Diemer K, Guo N, et al. PANTHER: a browsable database of gene products organized by biological function, using curated protein family and subfamily classification. Nucleic Acids Res 2003; 31: 334–41.

Vassilieva EV, Gerner-Smidt K, Ivanov AI, Nusrat A. Lipid rafts mediate internalization of beta1-integrin in migrating intestinal epithelial cells. Am J Physiol Gastrointest Liver Physiol 2008; 295: G965–76.

Wang L, Barylko B, Byers C, Ross JA, Jameson DM, Albanesi JP. Dynamin 2 mutants linked to centronuclear myopathies form abnormally stable polymers. J Biol Chem 2010; 285: 22753–7.

Wollscheid B, Bausch-Fluck D, Henderson C, O'Brien R, Bibel M, Schiess R, et al. Mass-spectrometric identification and relative quantification of N-linked cell surface glycoproteins. Nat Biotechnol 2009; 27: 378–86.

Woodhoo A, Alonso MB, Droggiti A, Turmaine M, D'Antonio M, Parkinson DB, et al. Notch controls embryonic Schwann cell differentiation, postnatal myelination and adult plasticity. Nat Neurosci 2009; 12: 839–37.

Yates JR 3rd, Eng JK, McCormack AL, Schieltz D. Method to correlate tandem mass spectra of modified peptides to amino acid sequences in the protein database. Anal Chem 1995; 67: 1426–36.

Zuchner S, Noureddine M, Kennerson M, Verhoeven K, Claeys K, De Jonghe P, et al. Mutations in the pleckstrin homology domain of dynamin 2 cause dominant intermediate Charcot-Marie-Tooth disease. Nat Genet 2005; 37: 289–94.